Target mass dependence of neutron emission in collisions with 35 MeV/nucleon ^{14}N ions

A. Kiss and F. Deák

Department of Atomic Physics, Eötvös University, H-1088 Budapest, Hungary

Z. Seres

Central Research Institute for Physics, H-1525 Budapest, Hungary

G. Caskey,[*] A. Galonsky, L. Heilbronn, and B. Remington[†]

National Superconducting Cyclotron Laboratory and Department of Physics and Astronomy, Michigan State University,
East Lansing, Michigan 48824

(Received 18 February 1988)

Energy and angular distributions of neutrons emitted from collisions of 35 MeV/nucleon ^{14}N ions with carbon, nickel, and holmium nuclei were measured. The neutrons were in coincidence with Li, Be, B, or C fragments at angles from 7° to 23° in the plane of the neutron detectors and at 15° out of this plane. Using fragment velocity bins of width corresponding to $E/A = 7$ MeV, we find the shapes of the neutron spectra above 15 MeV to be similar for the different targets for a given coincident fragment species, velocity bin, and angle. The cross sections are discussed in terms of moving thermal sources. In all cases the velocity and temperature parameters of the intermediate rapidity source are consistent with $E/A = 8.5 \pm 2.5$ MeV and $T = 9 \pm 2.5$ MeV, respectively. In agreement with a simple stripping-pickup model, the associated neutron multiplicities of this source decrease approximately linearly with the velocity of the coincident light fragments for fragment angles $\leq 15°$. Using the model to compute the mass of the source, we find that, with some fluctuations, these multiplicities are proportional to the mass. Also, the linear relationship is approximately the same for the three targets. The temperature parameters of the target-like source are between 1 and 3.5 MeV for all three targets, while the associated neutron multiplicities increase considerably with target mass. For colinear neutron-fragment coincidences for a given projectile-like isotope, the neutron multiplicities associated with the projectile-like source are about the same for all three targets, indicating that the average excitations of the parent fragments are similar.

I. INTRODUCTION

Investigations[1-10] of light-particle emission from intermediate energy (20 MeV $< E/A <$ 200 MeV) heavy-ion collisions have revealed that the particle spectra can be successfully parametrized using the assumption of thermal evaporation from moving hot sources. Systematics of the extracted parameters test the concept of local statistical equilibrium in heavy-ion collisions[11] and may give information on the temporal development and other characteristics of the heated zones.

To date, such studies have generally taken the form of inclusive measurements of light-particle spectra.[2,12-14] A clear picture of the target dependence on proton and light-particle yields has not yet emerged, though. At $E/A > 50$ MeV, yields tend to increase monotonically with target mass.[12,13] At lower energies ($E/A < 20$ MeV), the reverse occurs, at least for higher-energy ejectiles.[2] A very recent work[14] at $E/A = 15$ and 25 MeV bombarding energies suggests a mixture of the above two trends. Also, calculated results presented in that work imply that only the compound nucleus component is sensitive to the mass of the target nucleus.

The difficulty in extracting physical trends from inclusive measurements of charged particle spectra is twofold: (1) The inclusive nature of the experiments neces-

sarily means that the data include a large mix of reaction types. This makes a clean separation of the spectra into various components such as compound nucleus, projectile-like, target-like, or preequilibrium components, essentially impossible. (2) Although charged-particle measurements are attractive for their convenience, one must eventually deal with questions of Coulomb barrier and final-state interaction effects. The combination of these two difficulties has to date obfuscated the interpretation and understanding of reported target mass dependences.

We therefore have conducted a series of exclusive measurements on the target dependence of neutron emission. The exclusivity ensures that clean separation of the spectra into their various components is easily and unambiguously accomplished. Furthermore, there are no Coulomb barrier effects to be unraveled from our results. We are therefore able to make relatively model-independent observations of the target mass dependence on neutron emission.

We report here on an analysis of neutron spectra in coincidence with fragments of Li, Be, B, and C from three targets—carbon, nickel, and holmium. The projectile was ^{14}N at an energy of 35 MeV/nucleon. Some of the data for the nickel and holmium targets and an analysis emphasizing the dependencies of fit parameters

on fragment angle have already been given.[15] Here we fit all the Ni and Ho data and the C data as well. In addition, we use smaller fragment velocity (or energy/nucleon) bins so that we can study the dependence of the parameters on fragment velocity. Velocity, rather than energy, was the chosen variable because the shapes of our fragment velocity spectra were found to be similar to each other at a given angle,[16,17] but the energy spectra were not. Therefore, any dependence of reaction details on fragment kinetics will be one on velocity rather than energy.

After a brief description of the experiment, we present the spectra that were constructed from the event data. Next, the fit parameters of an intermediate rapidity (IR) (or half beam velocity) source and of a target-like fragment (TLF) source and their target mass dependences are examined. Finally, we discuss the characteristics and target mass dependence of the projectile-like fragment (PLF) source.

II. RESULTS OF DATA EVALUATION

The experiment[15] was conducted with the K500 cyclotron at the National Superconducting Cyclotron Laboratory at Michigan State University. The energy spectra of the neutrons were determined at $\pm 10°$, $\pm 30°$, $\pm 70°$, $\pm 110°$, and $\pm 160°$ in the horizontal plane by the method of time of flight. The coincident fragments were detected with Si telescopes at $+7°$, $-10°$, $+15°$, $-18°$, and $+23°$ in the plane of the neutron detectors and at $15°$ out of this plane directly below the beam axis.

The neutron spectra were constructed for coincident fragments of Li, Be, B, and C. The velocities of the coincident fragments were divided into four bins of width corresponding to 7 MeV/nucleon. The lowest bin range was 9–16 MeV/nucleon. For the $+23°$ telescope, where the use of a thinner (30 μm) ΔE detector allowed the identification of PLF's of even lower energy, a fifth bin was created: 4–9 MeV/nucleon for Li and Be and 5–9 MeV/nucleon for B and C.

Figures 1 and 2 show typical neutron spectra for the C, Ni, and Ho targets. In each figure the shapes of the three spectra, especially above 15 MeV, are very similar to each other even though the targets have widely different masses. The low-energy parts of the spectra, especially the enhancements in Fig. 2, are target dependent. For the nickel target the enhancement is less pronounced than for the holmium target, and for carbon it is quite small.

The colinear (target, Si telescope, and neutron detector on a straight line) and near-colinear spectra contain dominating contributions from neutron decay of excited fragments wherein the daughter fragment is the coincident PLF.[18,19] The peak structures between 15 and 40 MeV in Fig. 1 have this origin, and they occur with about the same relative strength for all three targets. For the colinear geometry, fragment-neutron relative velocity spectra[19] were created for daughter fragments of 12 different species, but the bulk of the data were for the seven isotopes ^{6}Li, ^{7}Li, ^{7}Be, ^{9}Be, ^{10}Be, ^{11}B, and ^{12}C. The results, not included in this report, again show that a major share

of the coincident neutrons come from decay of one or a few discrete states of the excited parent fragment. Regardless of whether the target was C, Ni, or Ho, the colinear relative velocity spectra for a given coincident isotope are similar to each other and to those previously constructed[19] for Ho.

For each of the elements, Li, Be, B, and C, Table I lists the relative contributions of individual isotopes to the colinear neutron-fragment coincidences at $-10°$. These values result from using fragments with energy above 9 MeV/nucleon and neutrons with energy above 4 MeV. We see from this table that the distribution amongst the isotopes of one element does not change drastically with target, but that there is a trend toward greater population
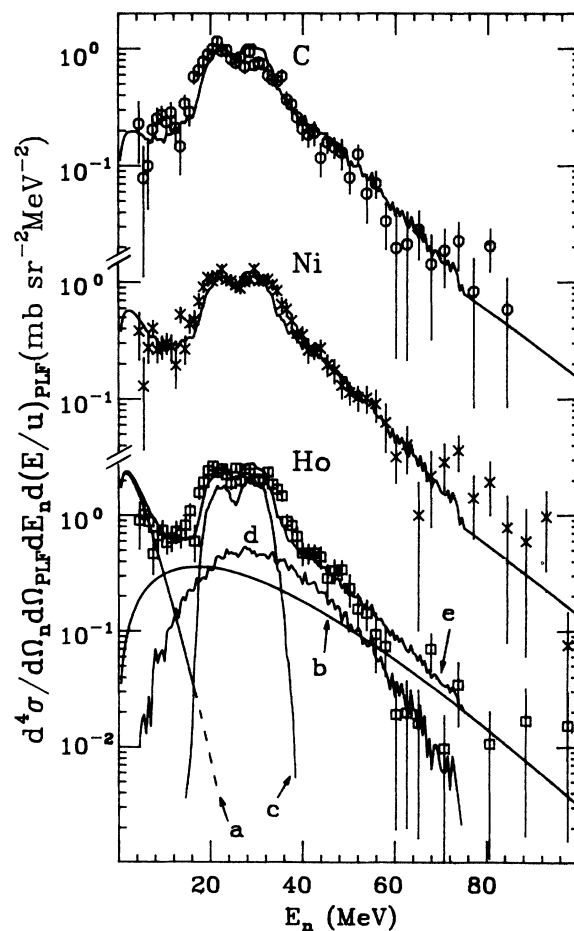

FIG. 1. Energy spectra of neutrons from the carbon, nickel, and holmium targets at $-10°$ in coincidence with projectile-like fragments of lithium at $-10°$ and within the 23–30 MeV/nucleon energy bin. The curves give the sum of the calculated contributions from three moving sources. The IR and TL source parameters (Table II) were determined from spectra at seven other angles. For the holmium target we also show the individual contributions—a from a target-like source, b from an intermediate-rapidity source, and c and d from a projectile-like source. c gives the part from the lowest neutron-unstable states of ^{7}Li and ^{8}Li, and d gives the thermal part. The fluctuations result from the Monte Carlo calculations used for c and d. The sum of the contributions is given by e.
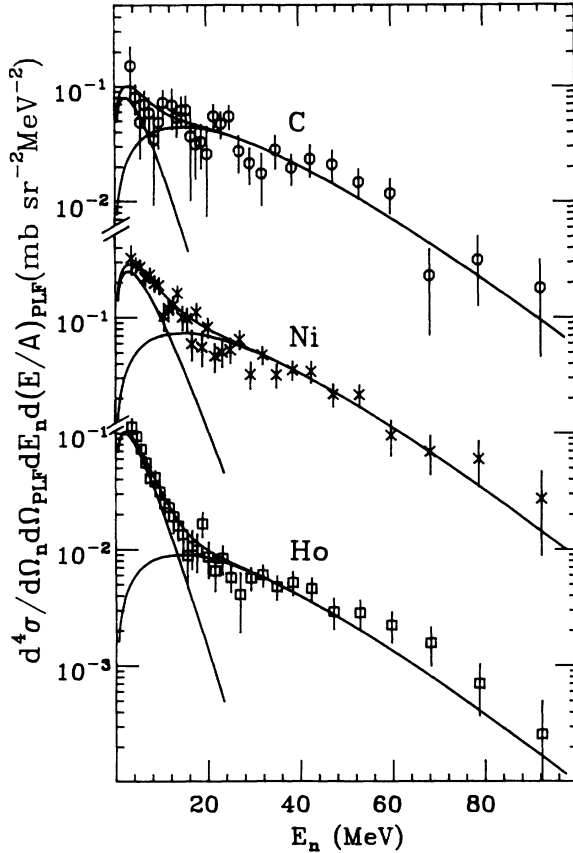
FIG. 2. Energy spectra of neutrons for the carbon, nickel, and holmium targets at $-30°$ in coincidence with lithium PLF's at $+23°$ and within the 9–16 MeV/nucleon energy bin. The curves show the contributions from the intermediate rapidity source (dominating at higher energies), from the target-like source, and from the sum of them. The source parameters (Table III) were determined from these spectra and from spectra at six other angles.

of the isotopes which are more neutron rich as the N/Z ratio increases. In general, this will produce a target-dependent effect on the shape of the colinear and near-colinear neutron energy spectra. In Fig. 1, however, where the coincident fragment is Li, the shapes of the PLF component are similar for the three targets. This is because here the decay energies from the lowest neutron unbound states of ^{8}Li (2.255 MeV) and ^{7}Li (7.456 MeV)—222 and 206 keV, respectively[20]—are almost equal.

III. TARGET MASS DEPENDENCE OF NONCOLINEAR NEUTRON EMISSION

A. Fit parameters of the IR and TLF sources

As in Refs. 15 and 16, the spectra of neutrons at the seven angles farthest from the angle of the coincident fragment (the noncolinear spectra) were fitted by two moving thermal sources, the IR source and the TLF source. The fit parameters were the kinetic energy/nucleon (E/A), the angle, the temperature, and the strength or multiplicity of each source. The parameter values for the fits shown in Figs. 1 and 2 are given in Tables II and III, respectively. (The multiplicity M of the IR or TLF source was obtained by dividing the coincidence cross section by the relevant fragment singles cross section.[15–17]) Such a fit was made for each of the six fragment angles, four fragment elements, and four or five fragment velocity bins, giving a total of about 100 fits for each target. We will refer to any of the 3×100 collections of data and the fit parameters as a "case." In a few cases, mostly where both fragment energy and angle were large, the statistics were poor and $(E/A)_{IR}$ was held fixed at the average value for the other bins of the same target, fragment element, and fragment angle. Although the concept of the TLF source may not have any clear physical meaning for a target nucleus as light as carbon, we

TABLE I. Isotope abundance distributions and relative neutron multiplicities. Each is for neutron-fragment coincidences with the $-10°$ colinear geometry for carbon, nickel, and holmium targets ($E_{PLF} \geq 9$ MeV/nucleon, $E_n \geq 4$ MeV). The relative multiplicities tell the number of neutrons which come from the parent of the indicated isotope for targets of nickel and holmium relative to the number for a target of carbon.

| PLF | Isotope abundance distributions | | | Relative neutron multiplicities | |
	Carbon (%)	Nickel (%)	Holmium (%)	$M(Ni)/M(C)$	$M(Ho)/M(C)$
^{6}Li	45 ±6	37 ±5	32 ±5	0.79±0.16	0.80±0.16
^{7}Li	54 ±7	59 ±8	61 ±8	0.67±0.47	0.73±0.47
^{8}Li	1.3±1	3.4±1.7	7.1±3.5		
^{7}Be	66 ±3	63 ±3	28 ±5		
^{9}Be	11 ±3	11 ±3	24 ±4	1.04±0.25	1.37±0.34
^{10}Be	23 ±3	26 ±3	48 ±4		
^{10}B	19 ±5	15 ±4	13 ±4	0.99±0.2	0.89±0.2
^{11}B	80 ±5	81 ±5	86 ±5	0.98±0.5	1.00±0.5
^{12}B	1.1±0.7	3.8±1.5	1.6±1		
^{11}C	12 ±3	14 ±3	6 ±3	0.98±0.18	0.34±0.2
^{12}C	76 ±6	73 ±6	82 ±6	0.92±0.18	0.81±0.17
^{13}C	12 ±3	14 ±3	13 ±3		

TABLE II. Parameter values of the IR and TL moving source contributions to the fits shown in Fig. 1.

Target		Strength $(mb/sr^{-2}MeV^{-2})$	E/A (MeV)	Temperature (MeV)	Angle (deg)
Carbon	IR source	9.6±0.9	10.1 ±1.2	9.3 ±0.4	8±3
	TL source	5.3±1.1	0.64±0.04	2.2 ±0.4	10±4
Nickel	IR source	13.7±0.9	7.4 ±1.4	9.5 ±0.6	3±1.4
	TL source	21.9±1.5	0.28±0.06	2.45±0.3	−4±3
Holmium	IR source	28 ±2	10.3 ±0.8	8.2 ±0.4	4±2
	TL source	108 ±4	0.13±0.02	2.4 ±0.1	5±2

needed the contribution from this kind of source for the description of the low energy parts of the spectra (see Fig. 2) and therefore included it.

For the IR source the values of E/A scattered around 8.5 MeV with a deviation of about 2.5 MeV. The values of temperature were roughly the same as the E/A values. The temperature values T_{IR} when the coincident fragments were at + 15° are shown in Fig. 3. There is no significant trend in the values for any of the target nuclei as a function of either the PLF energy/nucleon or the PLF identity. This was also true for coincident fragments at each of the other five angles where measured. The mean value of T_{IR} for the carbon target in Fig. 3 is around 7 MeV, which is somewhat lower than for the Ni and Ho targets. This result was independent of the angle of the PLF. All IR temperatures are consistent with an average value of 9±2.5 MeV. For the carbon and nickel cases the angle of the IR source scatters within the range ±10° without any conclusive favoring of either the same side or the side opposite the detected fragment. For the holmium target this parameter shows the same left-right asymmetry which was found and discussed earlier.[9,15,16]

For the TLF source the values of E/A were <1 MeV for the Ni and Ho targets[15,16] and <3 MeV for the C target. For all three targets the TLF angle generally had a sign opposite that of the detected fragment, but it scattered considerably in the range 0°–80°. Figure 4 compares the extracted TLF temperatures for C, Ni, and Ho targets when the fragment is at 15° out of the plane. For Ho most of the values are between 2 and 2.5 MeV, and for Ni between 2 and 3.5 MeV. For both targets the temperature drops with increasing fragment velocity. Comparison between these two targets for all of the cases has shown that, as in Fig. 4, the temperatures for Ni were, on

the average, somewhat (up to 20%) higher than those for Ho.[15] For the C target the contribution from the TLF source was always small, and therefore the source parameters were less well determined than for the heavier targets. Nevertheless, the temperature values are in the same range.

B. The stripping-pickup model

The $(E/A)_{IR}$ and T_{IR} values have been found not to depend on the identity, energy, or angle of the coincident fragment (see also Refs. 15 and 16). One may suppose that the IR neutron emission occurs at an early stage of the reaction, whereas the fragment departs later. This idea can be used to develop a stripping-pickup model[16] of peripheral collisions. This model offers a simplified view of a peripheral collision. First the participant zone develops in the interaction of an abraded part of the projectile with an approximately equal mass from the target nucleus. This zone emits the IR nucleons. Later the coincident PLF is formed from the projectile spectator by a decelerating mass pickup from the hot participant zone.

The kinematic consequences of this model can be evaluated without knowledge of the details of the dynamics. By the constraint of linear momentum conservation for the component in the beam direction an estimate can be made for the mass of the IR source, A_{IR}. Accordingly, in the first step, where the IR source is formed, the projectile drops off some nucleons on the target. Later ΔA nucleons are picked up. Momentum conservation gives

$$A_{proj}v_0 = A_{IR}v_{IR} + (A_{PLF} - \Delta A)v_0 ,$$

at the stripping, and when the PLF is formed it gives

TABLE III. Parameter values of the IR and TL moving source fits shown in Fig. 2.

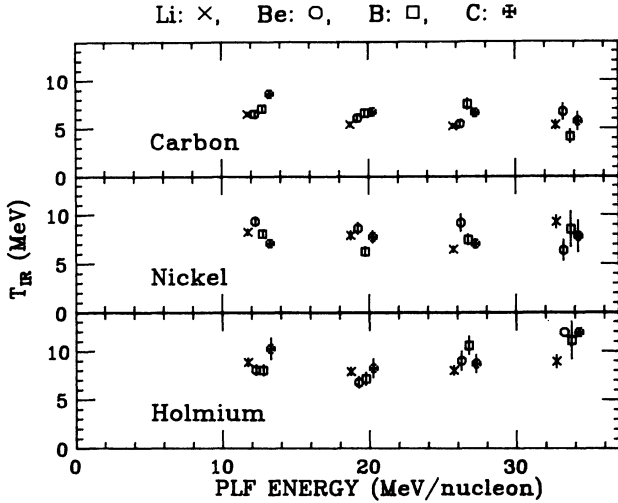| Target		Strength $(mb/sr^{-2}MeV^{-2})$	E/A (MeV)	Temperature (MeV)	Angle (deg)
Carbon	IR source	6.0±0.6	6.6 ±1.6	10.5±0.6	0±3
	TL source	3.4±1.0	0.5 ±0.2	2.6±1.2	−2±8
Nickel	IR source	9.6±0.6	6.5 ±1.3	10.4±0.6	1±2
	TL source	12.8±1.1	0.59±0.17	3.2±0.4	2±3
Holmium	IR source	11.7±0.8	6.3 ±1.1	10.3±0.5	2±3
	TL source	56.5±1.8	0.24±0.02	2.9±0.1	−13±3

Li: ×,   Be: ○,   B: □,   C: ✛

FIG. 3. Temperatures of the intermediate rapidity sources for carbon, nickel, and holmium targets with the coincident PLF's (symbols defined at top of figure) at 15°.

$$(A_{\text{PLF}} - \Delta A)v_0 + \Delta A v_{\text{IR}} = A_{\text{PLF}} v_{\text{PLF}} ,$$

where v_0, v_{IR}, and v_{PLF} are the lab. velocities of the incident ion, the IR source, and the PLF, respectively; and A_{proj} is the mass number (14 here) of the incident ion. The above equations may be solved for the unknowns ΔA and A_{IR}. Making an adjustment for the nonzero angles of the IR source and the PLF, we get for A_{IR}:

$$A_{\text{IR}} = \left[\frac{A_{\text{proj}} v_0}{v_{\text{IR}} \cos\theta_{\text{IR}}} + \frac{A_{\text{PLF}} v_0}{v_0 - v_{\text{IR}} \cos\theta_{\text{IR}}} \right]$$
$$- \left[\frac{v_0 A_{\text{PLF}}}{v_{\text{IR}} \cos\theta_{\text{IR}}(v_0 - v_{\text{IR}} \cos\theta_{\text{IR}})} \right] v_{\text{PLF}} \cos\theta_{\text{PLF}} .$$

(1)

For each case the quantities on the right side of this equation are known; hence, in the stripping-pickup model A_{IR} is determined. We cannot test the model directly through Eq. (1), since A_{IR} is not one of the fit parameters. However, we note that the temperature of the IR source seems to be independent of all PLF parameters. Therefore, M_{IR}, the source multiplicity, which *is* one of the fit parameters, should be proportional to A_{IR}. As v_{IR} does not vary significantly with PLF velocity, Eq. (1), which holds for peripheral collisions, i.e., for small PLF angles, then predicts that M_{IR} should be close to a linear function of v_{PLF}, which is proportional to $\sqrt{(E/A)}_{\text{PLF}}$. For each target Fig. 5 shows M_{IR} plotted against $\sqrt{(E/A)}_{\text{PLF}}$ for the cases where beryllium is the coincident fragment and where its angle is small enough for peripheral collisions to dominate. One sees a relationship close to the predicted linear one. Data for the other fragments look similar for PLF angles $\leq 15°$ for all three targets. This linearity is evidence in support of the validity of the stripping-pickup model.

If the data of Fig. 5 are extrapolated to very low values of v_{PLF}, namely to those at the Coulomb barriers, perhaps we should obtain IR multiplicities comparable to preequilibrium neutron multiplicities measured in central collisions.[21] Although Eq. (1) may not be valid at such low PLF velocities, linear extrapolations to 4.9 MeV, i.e., to $\sqrt{(E/A)}_{\text{PLF}} = 2.2$, for the Ho target yield $M_{\text{IR}} = 4.4$, 3.3, and 3.2 for $\theta_{\text{PLF}} = 7°$, $-10°$, and $15°$, respectively. With Ne projectiles at a somewhat lower velocity, viz., at 30 MeV/nucleon, but with the same target nucleus, Hilscher *et al.*[21] obtained a value of 2.9.

Now to test whether M_{IR} is indeed proportional to A_{IR}. Figures 6 and 7 show M_{IR} vs A_{IR} computed with Eq. (1) for the C, Ni, and Ho targets. The figures include all the cases where M_{IR} could be determined. In a few of the cases for the C target, Eq. (1) gave A_{IR} values slightly over 26 nucleons. Though unphysical, these points are included. In Fig. 6 we see a rough linear correlation for

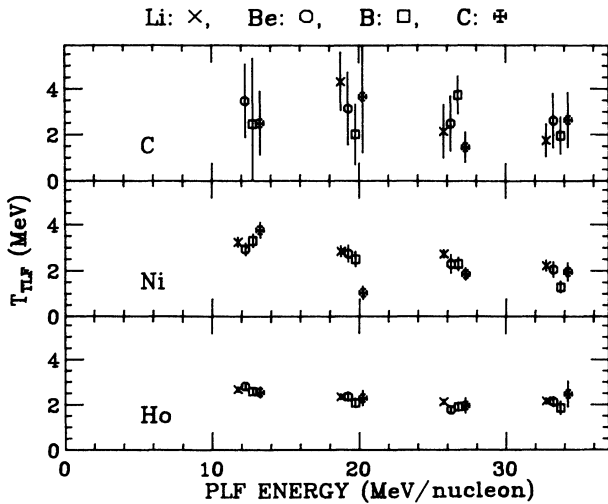Li: ×,   Be: ○,   B: □,   C: ✛

FIG. 4. Temperatures of the target-like sources for carbon, nickel, and holmium targets with the coincident PLF's (symbols defined at top of figure) at 15° out of plane.

Carbon: ○,   Nickel: ×,   Holmium: □

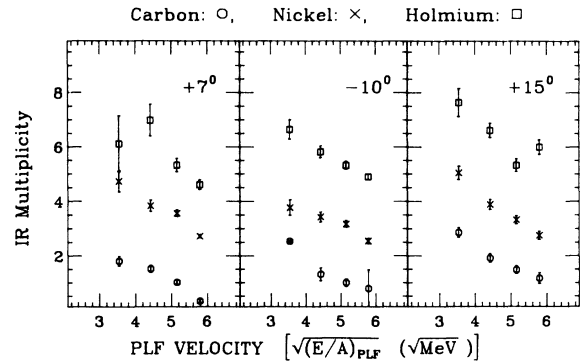PLF VELOCITY $\left[\sqrt{(E/A)}_{\text{PLF}} \; (\sqrt{\text{MeV}}) \right]$

FIG. 5. The IR multiplicities vs $\sqrt{(E/A)}_{\text{PLF}}$ for carbon, nickel, and holmium targets (symbols defined at top of figure) when the coincident PLF was beryllium at angles of $+7°$, $-10°$, and $+15°$. For the sake of clarity the Ni and Ho points have been displaced upward by two and four units, respectively. Otherwise, many of the points would overlap.

TARGET MASS DEPENDENCE OF NEUTRON EMISSION IN . . .

the $+7°$, $-10°$, $+15°$, and $15°$ out-of-plane cases. In Fig. 7 we see that the proportionality is not present for $\theta_{PLF} = +23°$, and all the points are at large values of A_{IR}. The results at 18° seem to represent the transition.

The slopes of the correlation in Fig. 6 are about the same for all three targets. The 15° in-plane and out-of-plane data for the C and Ni targets are close to each other, suggesting that any in-plane/out-of-plane asymmetry effects are smaller than the errors in the present data. For the Ho target, however, the multiplicities are about 25% higher for $\theta_{PLF} = +15°$ in the plane of the neutron detectors than for $\theta_{PLF} = 15°$ out of the plane. This is evidence that for the Ho target an in-plane/out-of-plane asymmetry exists in the neutron emission. This asymmetry is similar to asymmetries found for the same system but with coincident fragments at 30°,[16] and for light-particle emissions in other intermediate-energy heavy-ion collisions.[11] As all the multiplicities were determined with the assumption of isotropic neutron emission from the sources in their rest frames, the observed in-plane/out-of-plane asymmetry for the Ho target leads to an overestimate of the in plane and, with about the same

amount, to an underestimate of the out-of-plane M_{IR}. Consequently, it is possible that the Ho multiplicities are even closer to those for C and Ni than appears to be the case in Figs. 6 and 7.

The basic features of the IR source, i.e., its temperature and velocity as functions of θ_{PLF}, are about the same for all three targets. (And we note that the center of mass velocities are drastically different for the Ho and C targets.) Furthermore, for a given value of V_{IR}, the IR multiplicities for PLF angles $\leq 15°$ do not depend strongly on the PLF identity. One may conclude that for peripheral collisions we trigger on such coincidence events for which the first phase of the interaction is basically the same for the different target nuclei. The emission of the high-energy noncolinear neutrons, which have a coincident PLF, is consistent with a model in which only the overlapping zone of the colliding nuclei plays a decisive role in that emission. The identity and energy of the coincident PLF in peripheral collisions is determined by a later mass pickup by the light spectator from the participant zone.

The loss of correlation between M_{IR} and Eq. (1) estimates of A_{IR} for PLF angles $> 15°$ (Fig. 7) may be a sign that the reaction mechanism with which the PLF is produced has changed. This mechanism might also be connected mainly with the participant zones, as the behaviors of the multiplicities are again similar for the three targets.

We have evaluated M_{TLF}/M_{IR} ratios for all cases where the neutron multiplicities were available. The results show that the ratio is approximately independent of PLF angle and of PLF energy. We have found that for all three targets the ratio tends to be bigger for lighter coincident PLF's. M_{TLF}/M_{IR} lies between 6 and 3 for the Ho target (in-plane case) and between 2 and 1 for the Ni target. For the C target the ratio is less than 0.6.

C. Energy and momentum balance

Another aspect of the present type of data on neutron emission in coincidence with a light fragment is that we
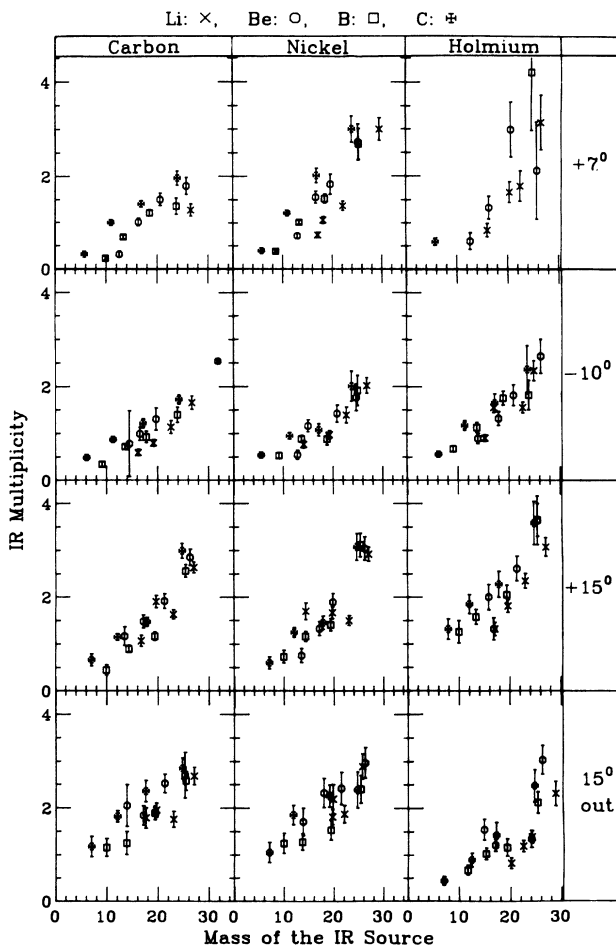
FIG. 6. Dependence of the IR multiplicity on the estimated mass of the participant zone for the carbon, nickel, and holmium targets for PLF angles $\leq 15°$. The values of A_{IR} were obtained from Eq. (1). Symbols for the PLF's are defined at the top.
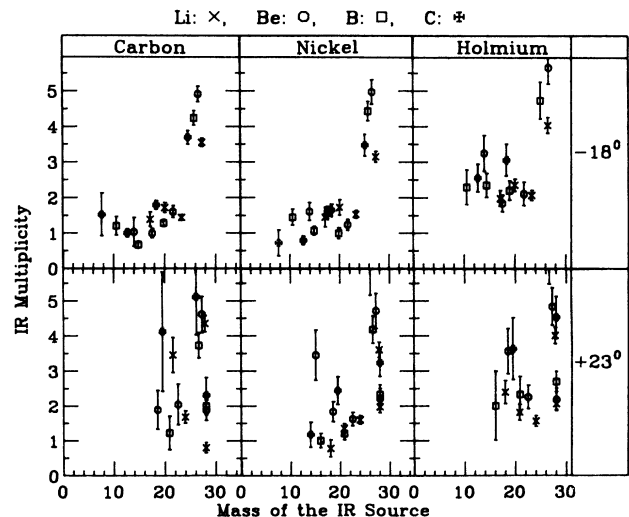
FIG. 7. Same as Fig. 6 for the 18° and 23° PLF angles.

can investigate whether or not the observed energy and momentum are conserved. A method for that was summarized by Eqs. (2) and (3) of Ref. 16.

The energy and momentum balances have been tested with the present data for the Ni and Ho targets. For the C target the formal use of Eqs. (2) and (3) gave the results that about 50–60 % of the incident energy and momentum are observed. However, with a C target the target-like source is just another excited light fragment from which a major share of the neutrons can be emitted via a few discrete particle-unbound states. Therefore, conclusions which use the assumption of Maxwellian distributions for the emitted particles may not be justified.

For the Ho target the ratios of the observed to incident energies and momenta were ≈ 1 with deviations up to 20% for all in-plane fragment angles, for all PLF velocity bins, and for all PLF elements. For $\theta_{PLF} = 15°$ out of the plane the ratios of the momenta were also close to 1, but for the energies the ratios scattered around 0.8. These results are consistent with what was found for $\theta_{PLF} = 10°$ and 30° in the plane and 30° out of the plane in Figs. 10 and 11 of Ref. 16. There, a similar phenomenon was qualitatively explained as a combined effect of an established in-plane/out-of-plane asymmetry in the IR multiplicity[11] and a possible rotation of the TLF source.

Typical results for the Ni target are shown in Fig. 8 for $\theta_{PLF} = -10°$; results for the other angles look similar. The observed momentum has values which average around the incident momentum to $\pm 20\%$. The observed energy, however, for all but one fragment element and angle, is smaller than the incident energy. The mean value of the energy ratio for the different fragment velocity bins is about 0.75, but it increases somewhat with fragment velocity. On the average, we miss an energy of about 100 MeV, which is a significant fraction of the incident energy.

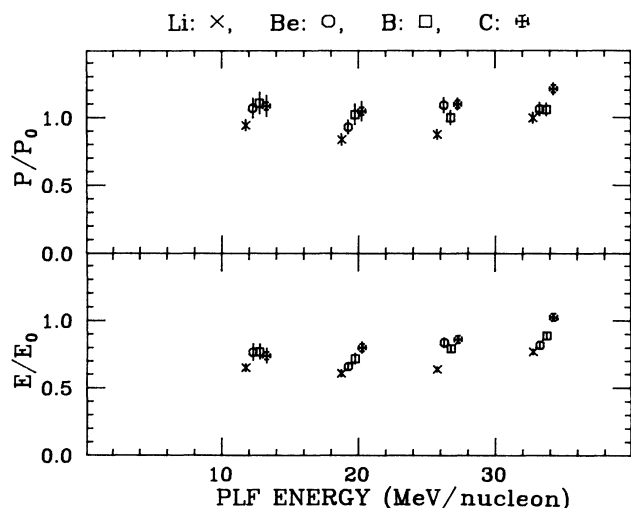As one can account for the incident momentum in the beam direction, the missing energy may be dissipated only by processes which, on the average, do not play an important role in the momentum balance. Unlike the Ho data, for Ni there is little, if any, in-plane/out-of-plane asymmetry, and a rotation could account for only a few MeV.[22] The enhanced probability for multifragmentation[11,23] in the case of the Ni target could be an explanation. According to one estimate,[24] the fission barrier of a nucleus near Ni is about 50–55 MeV, and therefore such a disintegration process could account for a large amount of energy. Perhaps a highly excited nickel-like system is formed at first; it quickly undergoes binary fission (or large-fragment emission) and then fragments of temperature around 3 MeV emit the neutrons from which we measure the average excitation.

IV. NEUTRON EMISSION FROM PROJECTILE-LIKE SOURCES

The neutron contribution from the PLF source was obtained from colinear and near-colinear spectra after subtraction of the calculated IR and TLF contributions computed from their fit parameters, which were determined from the neutron spectra at angles away from the colinearity condition. Each neutron spectrum from the PLF source was decomposed into two parts, one from decay of the excited fragment via discrete neutron unbound states with known energies, and another via many densely-packed states summing up to a Maxwellian distribution.[18,19] In several cases Monte Carlo calculations[19] were performed for the description of the colinear and near-colinear energy spectra of the neutrons as weighted sums of the contributions from the different isotopes. The abundances of the individual isotopes are listed on the left-hand side of Table I.

The curves in Fig. 1 give the spectra due to the TLF, IR, and PLF sources. For the Ho target we show the individual contributions. Curves c and d are results of empirically normalized Monte Carlo calculations. The twin peaks in curve c account for neutrons from forward and backward decay of the lowest neutron-unstable states of ^7Li and ^8Li (2.255 MeV and 7.456 MeV).[20] The broad bump, curve d, is the contribution from a Maxwellian source with 2.5 MeV temperature. The agreement between experiment and calculation in Fig. 1 is typical of all the cases. It is worth remembering that the curves are not just fits to the data of Fig. 1; curves a and b were computed with parameters determined from fitting spectra at seven noncolinear angles.

Accurate determination of the probability with which a particular PLF isotope emits neutrons involves several difficulties. Kinematic effects which are dependent on decay energy, the nonzero energy thresholds for the PLF's and for the neutrons, and side feeding from high-lying states of neighboring isotopes[25] are the most important sources of error. To study target dependence, however, it is sufficient to deal with relative rather than absolute multiplicities.

For the $-10°$ colinear data, the right-hand side of Table I displays neutron multiplicities from the Ni and Ho targets in comparison to those from the C target. Each multiplicity results from dividing the coincidence

Li: ×,   Be: ○,   B: □,   C: ⊕

FIG. 8. Ratios of the observed to incident momentum (upper part) and energy (lower part) for the nickel target with the coincident PLF at 10°.

cross sections for $(Z, A_{PLF}+1) \rightarrow n + (Z, A_{PLF})$ by the singles cross section for the production of $(Z, A_{PLF}+1)$. The entries in Table I are for the seven cases where the four required cross sections were measured. The errors quoted in Table I include, in addition to the statistical error, an uncertainty for isotope decomposition.[17] The latter error can be rather high in some cases. For example, the cross sections of ^{8}Li (which is always a small side-peak in the vicinity of a big ^{7}Li peak) have errors up to 50%. We assume that the factors which determine an absolute multiplicity from a relative multiplicity are the same for the different targets.

The relative multiplicities allow us to compare the degree of excitation of a given fragment for the different targets. The more a fragment is excited, the greater is the probability that the excitation energy exceeds the neutron separation energy, and the greater the number of coincident neutrons.[11,25] The many multiplicity ratios consistent with 1.0 in Table I indicate that the parent isotope comes out of the collision with an average excitation energy which is the same for the three targets. The only contrary case is ^{12}C* $\rightarrow$ ^{11}C $+ n$, where the relative multiplicity is only 0.3 for the Ho target but is ≈ 1 for the Ni target. However, in the case of ^{11}C $+ n$ we had to evaluate cross sections which were small relative to the neighboring ^{12}C $+ n$ cross sections[16] and the discrepancy in relative multiplicity could result from an error of decomposition into the two carbon isotopes.

V. CONCLUSIONS

For all fragment gates the noncolinear neutron spectra can be described in terms of an IR source and a TLF. The velocity and temperature of the IR source were consistent with $E/A = 8.5 \pm 2.5$ MeV/u and $T = 9 \pm 2.5$ MeV, respectively, without any significant dependence on whether the target was C, Ni, or Ho (or on any of the PLF parameters).

For a given fragment species and velocity the neutron multiplicity of the IR source is about the same for the three targets for all PLF gates. As predicted by a simple stripping-pickup model, the multiplicity decreases linearly with increasing velocity of the coincident fragment for all three targets at angles $\leq 15°$. At these angles the multiplicity is approximately proportional to the mass of the participant zone when the model is used to compute that mass.

The temperature of the TLF source was between 1.5 and 3.5 MeV for the Ni and Ho targets, showing a slight decrease with PLF velocity. The multiplicity ratio M_{TLF}/M_{IR} is approximately independent of the angle and energy of the coincident PLF, but it increases with target mass, being <0.6 for C, 1–2 for Ni, and 3–6 for Ho.

Tests for momentum and energy balance between the incident and observed values for the Ni and Ho targets show that we can approximately account for the momentum and for the energy with the Ho target. For the Ni target, however, there is a missing energy of about 100 MeV.

In many cases a colinear or near-colinear neutron spectrum is dominated by events from the decay of a few discrete neutron-unbound states of the parent of the detected projectile-like fragment. For the colinear geometry we find that the percentage abundance of the heavier isotopes of a given PLF element increases as the target mass increases. For each of these isotopes, however, the neutron multiplicity, within errors of about 20–60%, is the same for the three targets employed. Hence, the average excitation of the parent fragment does not depend critically on the target.

In summary then, for the projectile used here, 35 MeV/nucleon ^{14}N, the properties of the IR and PLF sources have little, if any, dependence on the target.

*Present address: Donnelly Corporation, Holland, MI 49423.
†Present address: Lawrence Livermore National Laboratory, Livermore, CA 94550.
[1]T. C. Awes, G. Poggi, S. Saini, C. K. Gelbke, R. Legrain, and G. D. Westfall, Phys. Lett. **103B**, 417 (1981).
[2]T. C. Awes, S. Saini, G. Poggi, C. K. Gelbke, D. Cha, R. Legrain, and G. D. Westfall, Phys. Rev. C **25**, 2361 (1982).
[3]B. B. Back, K. L. Wolf, A. C. Mignerey, C. K. Gelbke, T. C. Awes, H. Breuer, V. E. Viola, Jr., Phys. Rev. C **22**, 1927 (1980).
[4]T. C. Awes, G. Poggi, C. K. Gelbke, B. B. Back, B. G. Glagola, H. Breuer, V. E. Viola, Jr., and P. Dyer, Phys. Rev. C **24**, 89 (1981).
[5]M. B. Tsang, C. B. Chitwood, D. J. Fields, C. K. Gelbke, D. R. Klesch, W. G. Lynch, K. Kwiatkowski, and V. E. Viola, Jr., Phys. Rev. Lett. **52**, 1967 (1984).
[6]E. Holub, D. Hilscher, G. Ingold, U. Jahnke, H. Orf, and H. Rossner, Phys. Rev. C **28**, 252 (1983).

[7]H. Gemmeke, P. Netter, Ax. Richter, L. Lassen, S. Lewandowski, W. Lücking, and R. Schreck, Phys. Lett. **97B**, 213 (1980).
[8]G. A. Pettit, A. Gavron, J. R. Beene, B. Cheynis, L. R. Ferguson, F. E. Obenshain, F. Plasil, G. R. Young, M. Jääskeläinen, D. G. Sarantites, and C. F. Maguire, Phys. Rev. C **32**, 1572 (1985).
[9]G. Caskey, A. Galonsky, B. Remington, A. Kiss, F. Deak, and Z. Seres, Phys. Rev. C **31**, 1597 (1985).
[10]W. Lücking, R. Schreck, K. Keller, L. Lassen, A. Nagel, and G. Gemmeke, Z. Phys. A **320**, 585 (1985).
[11]C. K. Gelbke and D. H. Boal, Prog. Part. Phys. **19**, 37 (1987).
[12]B. Jakobsson, L. Carlen, P. Kristiansson, J. Krumlinde, A. Oskarsson, I. Otterlund, B. Schroder, H. A. Gustafsson, T. Johansson, H. Ryde, G. Tibell, J. P. Bondorf, G. Fai, A. O. T. Karvinen, O. B. Nielsen, M. Buenerd, J. Cole, D. Lebrun, J. M. Loiseaux, P. Martin, R. Ost, P. de Saintignon, C. Guet, E. Monnand, J. Mougey, H. Nifenecker, P. Perrin, J. Pinston, C.

Ristori, and F. Schussler, Phys. Lett. **102B**, 121 (1981).

[13]R. L. Auble, J. B. Ball, F. E. Bertrand, C. B. Fulmer, D. C. Hensley, I. Y. Lee, R. L. Robinson, P. H. Stelson, C. Y. Wong, D. L. Hendrie, H. D. Holmgren, and J. D. Silk, Phys. Rev. C **28**, 1552 (1983).

[14]R. L. Auble, J. B. Ball, F. E. Bertrand, R. L. Ferguson, I. Y. Lee, R. L. Robinson, and G. R. Young, Phys. Rev. C **37**, 390 (1988).

[15]B. A. Remington, G. Caskey, A. Galonsky, C. K. Gelbke, L. Heilbronn, J. Heltsley, M. B. Tsang, F. Deak, A. Kiss, Z. Seres, J. Kasagi, and J. J. Kolata, Phys. Rev. C **34**, 1685 (1986).

[16]F. Deak, A. Kiss, Z. Seres, G. Caskey, A. Galonsky, B. Remington, C. K. Gelbke, M. B. Tsang, and J. J. Kolata, Nucl. Phys. **A464**, 133 (1987).

[17]G. Caskey, L. Heilbronn, B. Remington, A. Galonsky, F. Deak, A. Kiss, and Z. Seres, Phys. Rev. C **37**, 969 (1988).

[18]A. Kiss, F. Deak, Z. Seres, G. Caskey, A. Galonsky, L. Heil-

bronn, B. A. Remington, and J. Kasagi, Phys. Lett. B **184**, 149 (1987).

[19]F. Deak, A. Kiss, Z. Seres, G. Caskey, A. Galonsky, and B. Remington, Nucl. Instrum. Methods **A258**, 67 (1987).

[20]F. Ajzenberg-Selove, Nucl. Phys. **A413**, 1 (1984).

[21]D. Hilscher, H. Rossner, A. Gamp, U. Jahnke, B. Cheynis, B. Chambon, D. Drain, C. Pastor, A. Giorni, C. Morand, A. Dauchy, P. Stassi, and G. Petitt, Phys. Rev. C **36**, 208 (1987).

[22]S. Cohen, F. Plasil, W. J. Swiatecki, Ann. Phys. **82**, 557 (1974).

[23]J. P. Bondorf, R. Donangelo, H. Schulz, and K. Sneppen, Phys. Lett. **162B**, 30 (1985).

[24]W. D. Myers and W. J. Swiatecki, Nucl. Phys. **81**, 1 (1966).

[25]J. Pochodzalla, C. K. Gelbke, W. G. Lynch, M. Maier, D. Ardouin, H. Delagrange, H. Doubre, C. Gregoire, A. Kyanowski, W. Mittig, A. Peghire, J. Peter, F. Saint-Laurent, B. Zwieglinski, G. Bizard, F. Lefebvres, B. Tamain, J. Quebert, J. P. Viyogi, W. A. Friedman, and D. H. Boal, Phys. Rev. C **35**, 1695 (1987).